Vibrational properties of alloys: Study of Si_xGe_{1-x}

Félix Yndurain*
Department of Physics,† University of California, Berkeley, California 94720
(Received 28 February 1977)

We have extended the theory of binary alloys developed by Falicov and Yndurain to study vibrational properties. As an example, the phonon density of states of amorphous Si_xGe_{1-x} alloys has been calculated for the entire range of concentrations. The results are in excellent agreement with first-order Raman spectra.

I. INTRODUCTION

In the last ten years there has been an increasing interest on the study of vibrational properties of noncrystalline materials like amorphous semiconductors, glasses, and alloys.[1] This has been mainly prompted by the fact that in noncrystalline materials light scattering gives information about phonon density of states in the entire frequency range. As an example, analysis of Raman spectra has identified the presence of homonuclear bonds[2] in amorphous SiC. Study of infrared and Raman spectra has given information on coordination, topological arrangement, and bonding character of some chalcogenide glasses[3] like Ge_xSe_{1-x} and Ge_xS_{1-x}. These experimental techniques have also been used to obtain information on phonon density of states of amorphous covalent semiconductors.[4] Finally, information about the phonon density of states of amorphous and crystalline semiconducting alloys has been obtained by means of first- and second-order Raman spectra.[5,6]

In spite of current interest and the rich experimental information on vibrational properties of noncrystalline materials, the theoretical situation is not satisfactory, most of the work being concerned with homopolar amorphous semiconductors.[7] The theoretical approaches used thus far to study vibrational properties of alloys can be classified in three categories: (a) numerical calculations on finite clusters with various boundary conditions[8]; (b) mean-field approximations like the averaged T matrix and coherent-potential approximations[9]; and (c) study of molecular units interacting weakly.[10] Each of these approaches is valid for very specific situations and its extension to more general cases is difficult. The results using (a) are appropriate when looking at the local density of states, since it is not very sensitive to boundary conditions when dealing with large enough clusters of atoms. This approach is also valid for studying mixed crystals[11] where periodic boundary conditions are appropriate. The main drawback of single-site mean-field approximations is their inability to take into account short-range-order effects. Finally molecular-type calculations are valid indeed for molecular systems only.

In this work we present a theoretical approach to study vibrational properties of alloys which we believe overcomes the shortcomings of previous approaches.[12] It is essentially based on the theory of Falicov and Yndurain intended to study the electronic properties of binary alloys.[13] In this theory the cluster–Bethe-lattice approximation[14,15] is used in such a way the short-range properties are present in both the cluster (exactly) and in the Bethe lattice (in an approximate form).

Although the theory we present here is general, we have applied it to study the phonon density of states of Si_xGe_{1-x} alloys because: (i) first-order Raman spectra have been measured for the entire range of concentrations[5] (see Fig. 1); (ii) the results have been checked against second-order Raman spectra and inelastic tunneling measurements.[6] In addition, the bonding character and coordination of both Si and Ge is very similar;

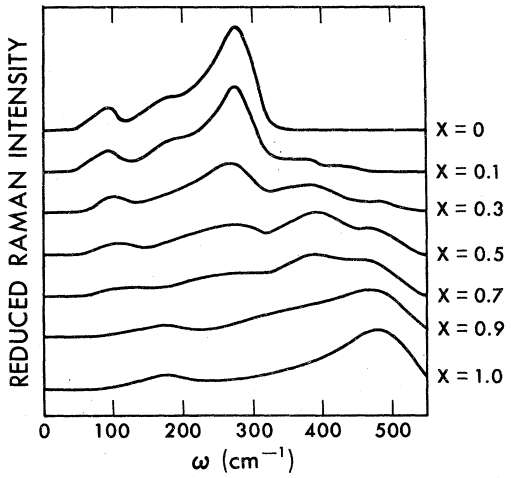

FIG. 1. Experimental reduced first-order Raman intensity vs frequency of amorphous Si_xGe_{1-x} alloys (Ref. 5). The curves are normalized to the same area. The concentration of Si atoms X is indicated in the right-hand side of the curves.

thus the distribution of Si and Ge atoms is expected to be rather homogeneous throughout the alloy.[16] Finally, since the ratio of ion masses is large ($m_{Ge}/m_{Si}=2.6$) the effects of short-range order and clustering should be clearly reflected in the phonon density of states.

In order to study the phonon density of states of Si_xGe_{1-x} alloys we will deal with the Born model.[17] In this model the potential energy is given by

$$V(\vec{r})=\tfrac{3}{4}\beta\sum_{l\Delta}[(\vec{u}_l-\vec{U}_{l\Delta})\cdot\vec{r}_{l\Delta}(l)]^2 + \tfrac{1}{4}(\alpha-\beta)\sum_{l\Delta}(\vec{u}_l-\vec{u}_{l\Delta})^2 . \quad (1)$$

The sums are on atoms l and their nearest neighbors $l\Delta$; $\vec{r}_\Delta(l)$ is the unit vector from the equilibrium position of atom l to that of its neighbor $l\Delta$, and $\vec{u}_l$ and $\vec{u}_{l\Delta}$ are the displacement vectors of these atoms. In this model we can identify a central force, of strength $2\beta+\alpha$, and a noncentral one of strength $\alpha-\beta$. In this work we assume that the potential-energy parameters α and β in (1) are the same for all pairs of atoms (Si-Si, Ge-Ge, and Si-Ge). This is justified by the fact that the bonding character of both Si and Ge is very similar.

The format of this paper is as follows. In Sec. II we discuss the extension of the cluster–Bethe-lattice approximation to study vibrational properties of alloys. In Sec. III we present phonon densities of states corresponding to clusters of different size for a fixed concentration. The density of states for different concentrations is calculated and a detailed comparison with experiments is presented as well. Finally, in Sec. IV some conclusions are drawn.

II. CLUSTER-BETHE-LATTICE APPROXIMATION

In addition to the concentration X, we characterize the alloy by the short-range-order parameter P_A (P_B) which gives the probability that when choosing a nearest-neighbor pair such that one of the atoms is of class A (B), the other atom is of the same class.[13] In this section we mostly discuss the Bethe lattice because once we know how to solve it, the extension to obtain the density of states for the cluster–Bethe-lattice system is straightforward.[14] The density of states in the Bethe lattice corresponding to both the binary compound and segregation sequences defined in Ref. 13 is easy to obtain. For these sequences the short-range-order parameters take the simple form

$$P_A=P_B=1 \quad \text{(segregation sequence)}, \quad (2a)$$

$$\left.\begin{aligned} P_A&=0,\quad P_B=(X_B-X_A)/X_B \quad \text{if } X_A\le X_B \\ P_B&=0,\quad P_A=(X_A-X_B)/X_A \quad \text{if } X_B\le X_A \end{aligned}\right\}$$

(binary-compound sequence). (2b)

Then we get the following equation for the matrix elements of the Green's function G associated with the atom in which we are interested.

(i) Segregation sequence: If the reference atom is, say, of kind A we obtain

$$M_A\omega^2\underline{G}_{0,0}=\underline{1}+\underline{D}_1\cdot\underline{T}_A\cdot\underline{G}_{0,0}+\sum_{i=2}^{4}\underline{D}_i\cdot\underline{S}_i\cdot\underline{T}_A\cdot\underline{G}_{0,0}\cdot\underline{S}_i , \quad (3)$$

where the transfer matrix $\underline{T}$ is given by

$$M_A\omega^2\underline{T}_A=\underline{D}_1+\underline{D}_0\cdot\underline{T}_A+\sum_{i=2}^{4}\underline{D}_i\cdot\underline{S}_i\cdot\underline{T}_A\cdot\underline{S}_i\cdot\underline{T}_A . \quad (4a)$$

In these equations M_A represents the mass of ions of class A; ω stands for the frequency. The matrices $\underline{D}$ are formed by the matrix elements of the full dynamical matrix as described in detail in Ref. 18. Finally the matrices $\underline{S}$ correspond to the

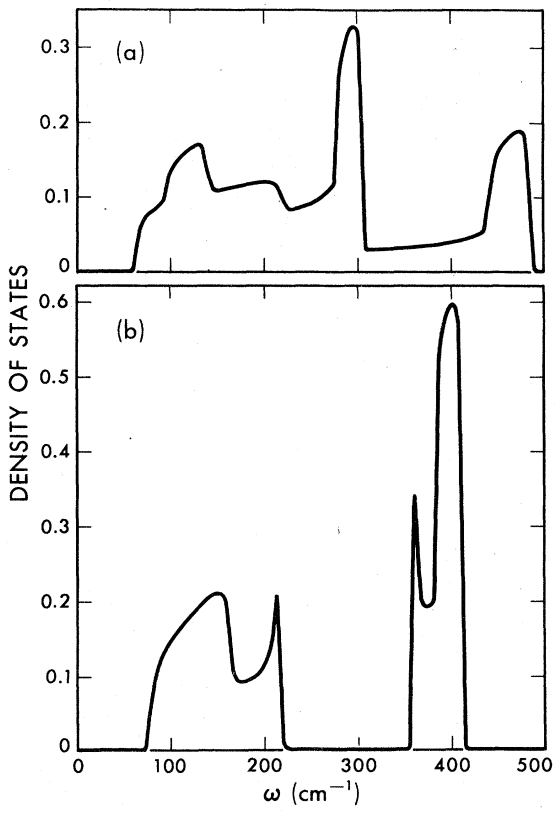

FIG. 2. Total phonon density of states vs frequency for the Si_xGe_{1-x} alloy. (a) Segregation sequence (i.e., $P_{Si}=P_{Ge}=1$). (b) Binary compound sequence (i.e., $P_{Si}=P_{Ge}=0$).

symmetry operations of the tetrahedral coordination.

Once the matrix $\underline{G}_{0,0}$ is known, the local density of modes associated to the reference atom is given by

$$n_0^A(\omega) = -(\omega/\pi) M_A \,\mathrm{Im}[\mathrm{Tr}(\underline{G}_{0,0})] . \tag{5}$$

The total density of states corresponding to this sequence and for $X = 0.5$ is drawn in Fig. 2(a).

(ii) Binary-compound sequence: For this sequence we obtain

$$M_A \omega^2 \underline{G}_{0,0} = \underline{1} + \underline{D}_1 \cdot \underline{T}_1 \cdot \underline{G}_{0,0} + \sum_{i=2}^{4} \underline{D}_i \cdot \underline{S}_i \cdot \underline{T}_1 \cdot \underline{G}_{0,0} \cdot \underline{S}_i , \tag{6}$$

where now the transfer matrix $\underline{T}_1$ is given by

$$M_B \omega^2 \underline{T}_1 = \underline{D}_1 + \underline{D}_0 \cdot \underline{T}_1 + \sum_{i=2}^{4} \underline{D}_i \cdot \underline{S}_i \cdot \underline{T}_2 \cdot \underline{S}_i \cdot \underline{T}_2 , \tag{7a}$$

$$M_A \omega^2 \underline{T}_2 = \underline{D}_1 + \underline{D}_0 \cdot \underline{T}_2 + \sum_{i=2}^{4} \underline{D}_i \cdot \underline{S}_i \cdot \underline{T}_1 \cdot \underline{S}_i \cdot \underline{T}_i . \tag{7b}$$

To obtain the density of states associated with atoms of class B we have to change M_A into M_B, and $\underline{T}_1$ into $\underline{T}_2$ in (6). The total density of states corresponding to this sequence for $X = 0.5$ is drawn in Fig. 2(b).

For a general value of the short-range-order parameters P_A and P_B different from the above discussed, we use an interpolation scheme. In particular, in the case of the random distribution of atoms, the interpolation scheme for the Bethe lattice reduces to the virtual-crystal approximation in which all the atoms are equivalent (no short-range order), and their mass is given by

$$\overline{M} = X M_A + (1 - X) M_B . \tag{8}$$

In this case, we get the following equation for a one-atom cluster–Bethe-lattice system:

$$M_A \omega^2 \underline{G}_{0,0} = \underline{1} + \underline{D}_1 \cdot \overline{\underline{T}} \cdot \underline{G}_{0,0} + \sum_{i=2}^{4} \underline{D}_i \cdot \underline{S}_i \cdot \overline{\underline{T}} \cdot \underline{S}_i \cdot \underline{G}_{0,0} , \tag{9}$$

where $\overline{\underline{T}}$ is given by

$$\overline{M} \omega^2 \overline{\underline{T}} = \underline{D}_1 + \underline{D}_0 \cdot \overline{\underline{T}} + \sum_{i=2}^{4} \underline{D}_i \cdot \underline{S}_i \cdot \overline{\underline{T}} \cdot \underline{S}_i \cdot \overline{\underline{T}} . \tag{10a}$$

Since we are aiming to introduce short-range order, the density of states for this sequence depends on the cluster of atoms we are dealing with when the cluster-Bethe approximation is used. We leave the detailed discussion of this sequence to Sec. III.

Before we discuss the results of our calculation, we would like to comment on the way we obtain the transfer matrices. As it was shown in Ref. 18, the solution of (4a) or (10a) is reduced to solving a quartic equation. The solution of the transfer matrices in the case of the binary compound sequence (7a) and (7b) can be obtained from the solution of (4a) by a suitable transformation.[19] The problem of this kind of solution is that out of the continuum the choice of the proper root of the quartic equation is not simple, and one can get spurious solutions. Here instead we resort to a simple iterative procedure.[20] We can write T_A and $\overline{T}$ in the form

$$\underline{T}_A = \left(\underline{1} M_A \omega^2 - \underline{D}_0 - \sum_{i=2}^{4} \underline{D}_i \cdot \underline{S}_i \cdot \underline{T}_A \cdot \underline{S}_i \right)^{-1} \cdot \underline{D}_1 \tag{4b}$$

and

$$\overline{\underline{T}} = \left(\underline{1} \overline{M} \omega^2 - \underline{D}_0 - \sum_{i=2}^{4} \underline{D}_i \cdot \underline{S}_i \cdot \overline{\underline{T}} \cdot \underline{S}_i \right)^{-1} \cdot \underline{D}_1 . \tag{10b}$$

$\underline{T}_1$ and $\underline{T}_2$ in (7) can be written in a similar form. The solution of (4b) and (10b) can be easily obtained numerically by iteration. Details of this procedure are given in Ref. 20. The advantage of this way of solving the transfer matrices is that it ensures us to be in the right sheet of the Riemann's surface.

III. RANDOM ALLOY: COMPARISON WITH EXPERIMENTS

If we now try to reproduce the experimental results shown in Fig. 1, we realize that neither the segregation sequence [Fig. 2(a)] or the binary compound sequence [Fig. 2(b)] are appropriate. The density of states corresponding to the segregation sequence reproduces the peaks at ~280 and 480 cm^{-1} of the experimental Raman spectra but does not reproduces the peak at ~390 cm^{-1}. On the other hand the density of states corresponding to the binary compound sequence reproduces this peak but does not give the former ones.

In order to pick up the proper values of P_A and P_B in the $\mathrm{Si}_x\mathrm{Ge}_{1-x}$ alloy, we first study the one-atom cluster–Bethe-lattice system. As we said before, to solve the Bethe lattice for nonspecial values of the short-range parameters, we use an interpolation scheme in which the actual mass of the ion is approximated by an averaged mass. First of all, since we expect an homogeneous distribution of Si and Ge atoms, we shall assume that $P_{\mathrm{Si}} = P_{\mathrm{Ge}} = P$. If the central atom is of kind, say A, the mass of the atoms in the different shells of atoms as we go away from the center of the Bethe lattice are

$$M_0 = M_A, \quad M_1 = PM_A + QM_B, \quad M_2 = (P^2 + PQ)M_A + (Q^2 + QP)M_B,$$
$$M_3 = (P^3 + QP^2 + Q^3 + Q^2P)M_A + (Q^2P + QP^2 + P^2Q + Q^2P)M_B, \tag{11}$$
$$\vdots \qquad \vdots \qquad \vdots$$

when $Q = 1 - P$. To solve for the density of states in the Bethe lattice we write the local Green's function in a continued fraction form, such that the successive terms in the fraction contain the mean masses $M_1, M_2, \ldots$. The solution of this continued fraction cannot be obtained analytically, but the numerical solution is rather simple.

In Fig. 3 we show the density of states for the one-atom Bethe-lattice system for $P_{Si} = P_{Ge} = 0.5$. The position of the high frequency peaks as a function of the short-range-order parameter are also drawn in the insets of this figure.

In the inset of Fig. 3(a), we see that for $P_{Ge} = 1$ (Ge-Ge bond) we obtain a peak at ~290 cm^{-1} in accordance with Fig. 2(a). In the same way the inset on Fig. 3(b) indicates a peak at ~470 cm^{-1} corresponding to $P_{Si} = 1$ (Si-Si bond). Finally for $P_{Si} = P_{Ge} = 0$, there is a peak at ~400 cm^{-1} corresponding to the Si-Ge bond. The positions of these peaks are in agreement with the experimental data. Nevertheless it does not seem to be a preferred short-range order in Si_xGe_{1-x} alloys. In what follows we shall then adopt the values corresponding to the random distribution, i.e., $P_{Si} = P_{Ge} = 0.5$.

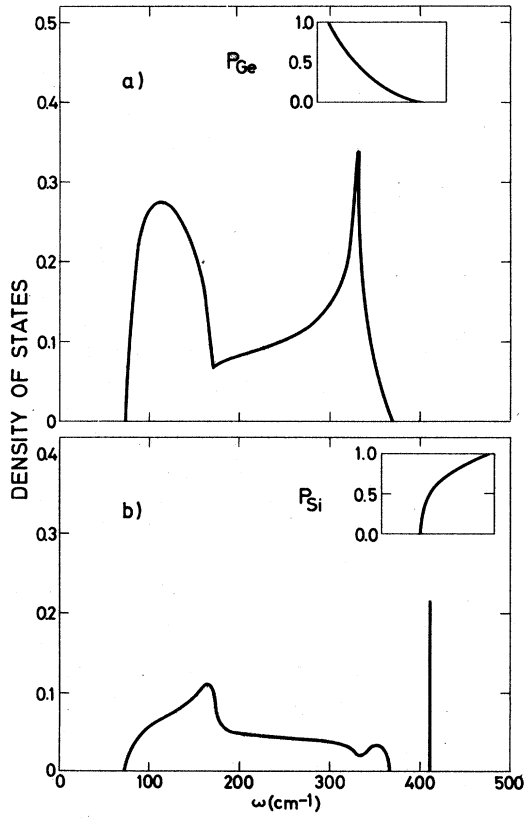

FIG. 3. Local density of states for the one-atom Bethe-lattice system. $P_{Si} = P_{Ge} = 0.5$. (a) Ge Bethe lattice; (b) Si Bethe lattice. The insets indicate the position of the high-frequency peaks as a function of the short-range-order parameter (see text).

We have calculated the density of states of the five-atom (the central atom plus its four nearest neighbors) cluster–Bethe-lattice system taking into account all possible cluster configuration and for the entire range of concentrations. The results when the central atom is Si and $X = 0.5$ are drawn in Fig. 4. The results corresponding to Ge and $X = 0.5$ are drawn in Fig. 5.

In order to compare with the experimental results we have calculated the weighted averages of the densities of states corresponding to the central atom in the five-atom cluster–Bethe-lattice system. The density of states is now given by

$$n_0(\omega) = \sum_C W_C n_0(\omega, c), \tag{12}$$

where all possible clusters C contribute each with its proper weight W_C given by

$$\begin{aligned}
&\text{Si-SiSiSiSi}, \quad W = X^5,\\
&\text{Si-SiSiSiGe}, \quad W = 4X^4(1-X),\\
&\text{Si-SiSiGeGe}, \quad W = 6X^3(1-X)^2,\\
&\text{Si-SiGeGeGe}, \quad W = 4X^2(1-X)^3,\\
&\text{Si-GeGeGeGe}, \quad W = X(1-X)^4,\\
&\text{Ge-GeGeGeGe}, \quad W = (1-X)^5,\\
&\text{Ge-GeGeGeSi}, \quad W = 4(1-X)^4X,\\
&\text{Ge-GeGeSiSi}, \quad W = 6(1-X)^3X^2,\\
&\text{Ge-GeSiSiSi}, \quad W = 4(1-X)^2X^3,\\
&\text{Ge-SiSiSiSi}, \quad W = (1-X)X^4.
\end{aligned} \tag{13}$$

The results for the whole range of concentrations are given in Fig. 6.[12] The shaded regions describe localized discrete states. To make them visible, we have added a small (8 cm^{-1}) imaginary component to the frequency.

A direct comparison of Figs. 1 and 6 reveals

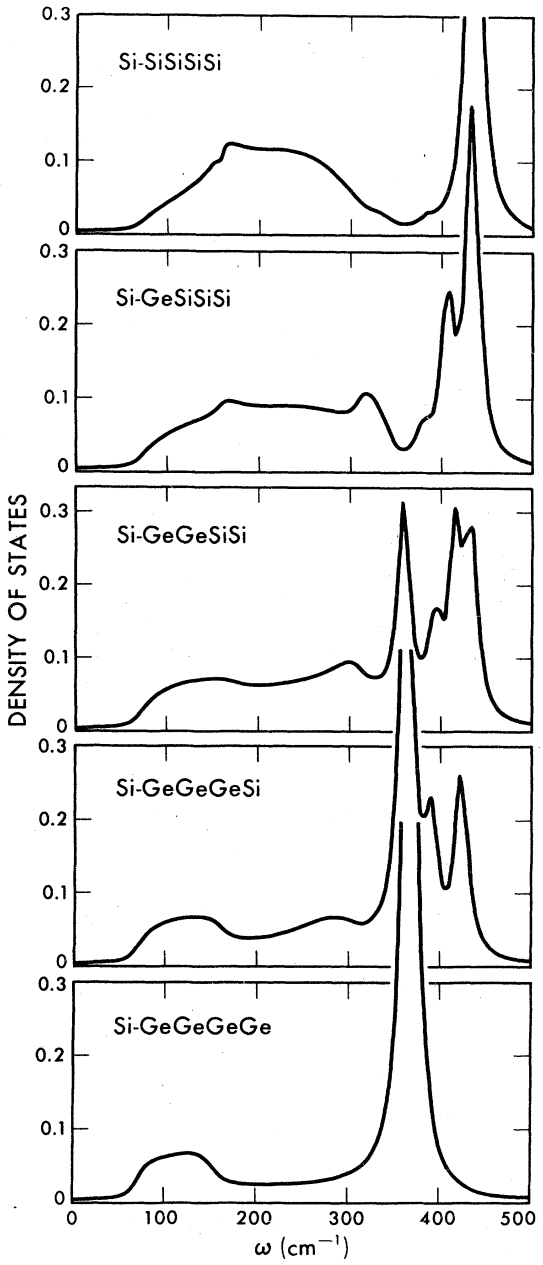

FIG. 4. Local phonon density of states corresponding to the central atom (Si in this case) of the five-atom cluster–Bethe lattice system for $X=0.5$. The distribution of atoms in the cluster is indicated. A small (8 cm^{-1}) imaginary contribution to the frequency has been added.

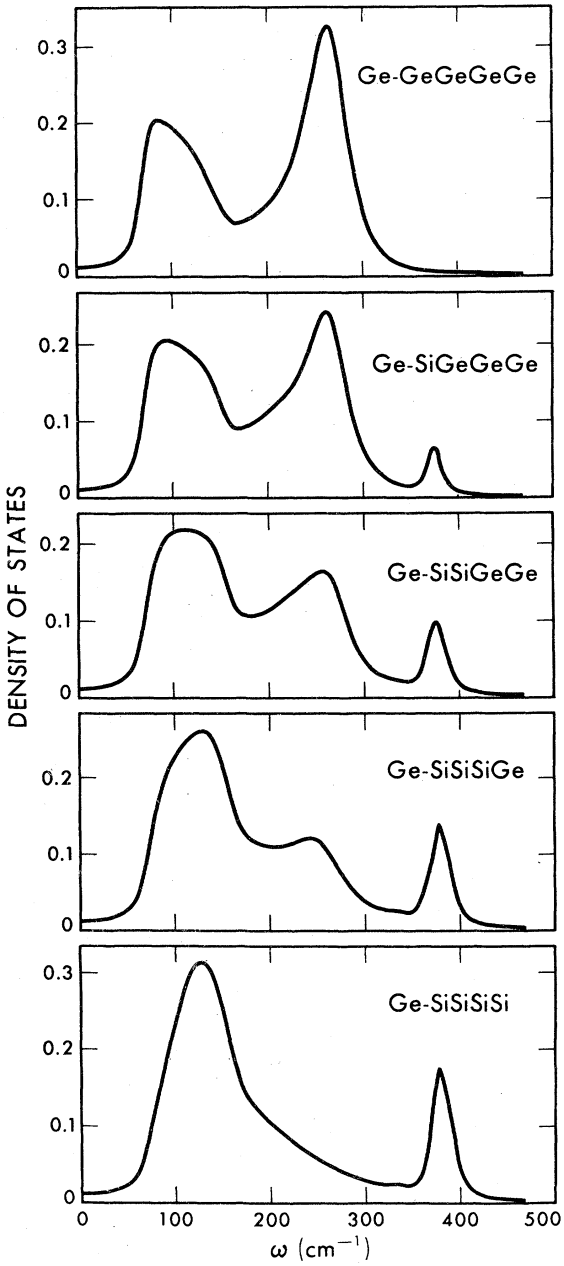

FIG. 5. Local phonon density of states corresponding to the central atom (Ge in this case) of the five-atom cluster–Bethe lattice system for $X=0.5$. The distribution of atoms in the cluster is indicated. A small (8 cm^{-1}) imaginary contribution to the frequency has been added.

good agreement with the experimental measurements. It should be noted that we just calculate phonon density of states but we do not even estimate matrix elements for Raman scattering. This allows us to compare the position of peaks but not their absolute strength.

The main features of the Raman spectra are reproduced in our calculation in the following ways:

(a) There is a peak at about 280 cm^{-1} whose strength decreases as the concentration of Si increases. The peak disappears at $X \simeq 0.7$ in both theory and experiment. Moreover the peak shifts to low frequencies as measurements by Feldman

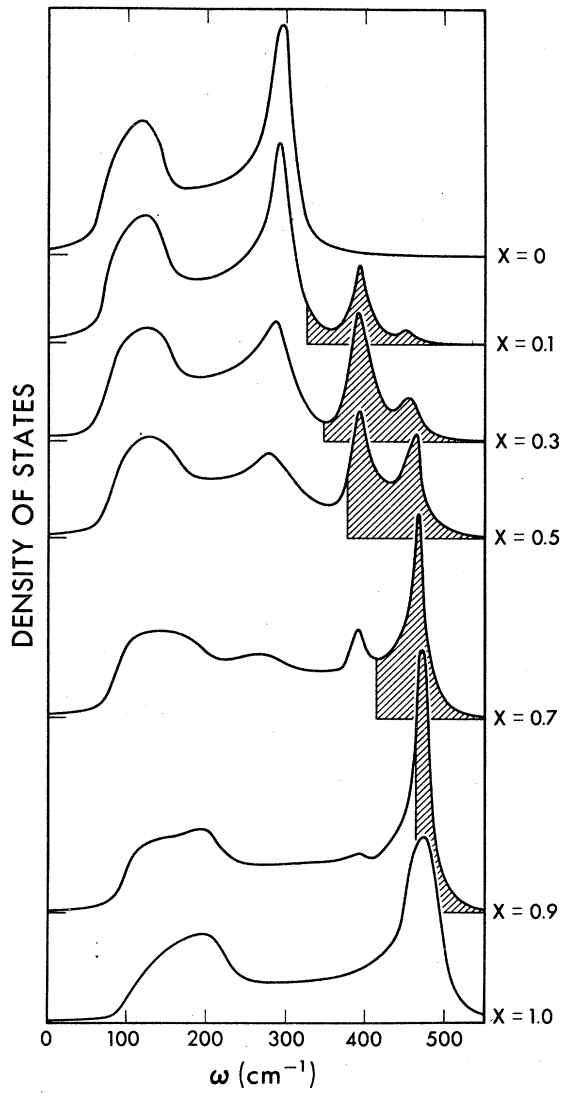

FIG. 6. Calculated total phonon density of states of amorphous Si_xGe_{1-x} alloys. The concentration of Si atoms X is indicated in the right-hand side of the curves. Shaded regions correspond to discrete localized states. A small (8 cm^{-1}) imaginary contribution has been added.

et al. indicate.[21] We interpret this peak as due to the presence of Ge-Ge bonds, as is apparent from the analysis of the individual five-atom clusters (see Fig. 4).

(b) There is another peak at about 470 cm^{-1} whose strength in the experiments decrease with the Si concentration. In our calculation, the height of this peak does not decrease with X, but the fraction of states associated with it does. This peak is due to the presence of Si-Si bonds (see Fig. 5). The modes associated with it are localized for concentrations of Si atoms less than ~0.9. For concentrations less than ~0.3 it is barely seen.

(c) A peak which is not present in either pure Si or Ge appears for all intermediate concentrations at ~380 cm^{-1}. This peak is due to the presence of Si-Ge bonds [see Figs. 2(b), 4, and 5] in the alloy and the modes associated with it are mostly localized (~90%) in the Si atoms. Although the position of this peak is almost independent of the concentration in our calculation, there is some experimental evidence[21] that it shifts from 389 to 402 cm^{-1} for $0<X<0.33$. The modes associated with this peak become localized when $X<0.6$.

(d) The low-frequency (<250 cm^{-1}) part of the spectrum cannot be discussed in detail because the matrix elements involved in the Raman scattering at those frequencies are small.[22] Nonetheless the trends in our calculation also agree with the experimental observations. We note that the peak at ~100 cm^{-1} for $X=0$ does not shift its position very much for $0<X<0.9$, but at $x\gtrsim 0.9$ it shifts to essentially its value for pure Si. The origin of this behavior is the presence of Ge-Si bonds which give rise to a peak at about 140 cm^{-1} [see Figs. 2(b) and 5], close to the pure Ge lower peak position. The modes associated with the former are mostly localized at the Ge atom, and are resonance modes throughout the entire range of concentrations. The particular positions of the low-frequency peaks of the Ge-Ge, Ge-Si, and Si-Si bonds are also responsible for the rather flat line shape of this feature at $X\cong 0.7$.

In order to check the above discussed results and to study how the results depend on the size of the cluster, we have calculated for $X=0.5$ the density of states corresponding to the 17-atom cluster shown in Fig. 7.

Since for a 17-atom cluster the combinatoried

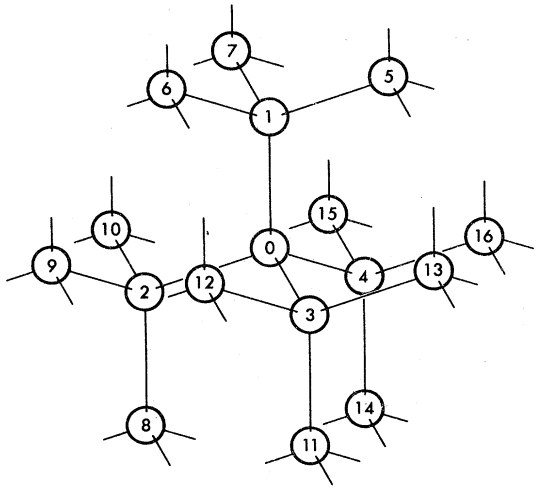

FIG. 7. 17-atom cluster with tetrahedral coordination. Central atom has label 0.

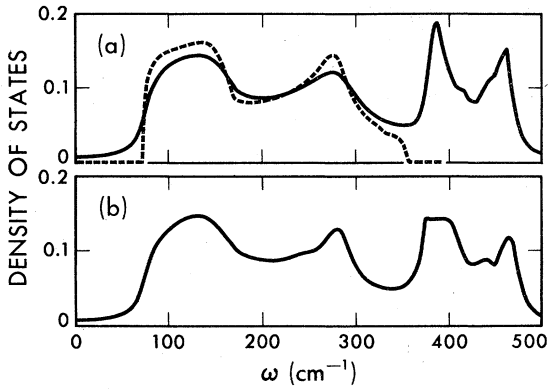

FIG. 8. Total phonon density of states vs frequency for the random sequence and $X=0.5$. (a) Five-atom cluster total density of states with an imaginary (8 cm^{-1}) contribution to the frequency has been added (solid line) without imaginary contribution to the frequency (broken line). (b) 17-atom cluster total density of states. The density of states has been obtained by averaging over a random selection of clusters (52 altogether). A small (8 cm^{-1}) imaginary contribution to the frequency has been added.

aspects of calculating the weight W_C as well as the sheer number of different clusters to consider makes the calculation impractical, we resort to a random selection of clusters (52 altogether). The averaged density of states corresponding to our random sampling is shown in Fig. 8(b) along with the exact weighted average corresponding to the 5-atom cluster. We notice immediately that the main features are common to both densities of states making the 5-atom cluster results reliable, and stressing the importance of short-range order.

The above discussed results apply to amorphous samples since no long-range order is assumed. Nevertheless they are also in good agreement with the results obtained by means of second-order Raman[6] scattering and electron tunneling[23] for crystalline alloys. These experimental results indicate that the phonon density of states of crystalline alloys present additional fine structure with respect to that of the amorphous samples. This new structure is essentially a peak at about 340 cm^{-1} close to a dip at about 360 cm^{-1}. Looking at the second and third panels of Fig. 3 we see that this structure may be due to the simultaneous presence of Si-Ge and Si-Si bonds. To check this we have calculated the density of states of two different configurations in the 17-atom cluster of Fig. 7. Both clusters are such that the central atom is Si with two Si nearest neighbors and two Ge nearest neighbors. In the first cluster the distribution of Si and Ge atoms in the second-nearest-neighbors shell is random, whereas in the second cluster the distribution is such that all the atoms are surrounded by two atoms of its own kind and two of the other kind. The density of states corresponding to the first cluster is shown in Fig. 9(a) and that corresponding to the second cluster is shown in Fig. 9(b). From this result we can tentatively conclude that the presence of clusters of the type *A-ABAB* enhances the appearance of a dip at around 350 cm^{-1}. This does not imply however any specific short-range order in crystalline alloys. On the contrary, the overall shape of the experimental curves[6] indicate that in crystalline Si_xGe_{1-x} alloys the distribution of atoms is essentially random as in the amorphous case.

IV. CONCLUDING REMARKS

In this work we have calculated the vibrational properties of Si_xGe_{1-x} alloys for the entire range of concentrations. The method of calculation allows us to include short-range order and keep tetrahedral coordination throughout the entire system. Based on our results we can conclude the following:

(i) Statistics of the near-neighbor coordination must be explicitly dealt with, while further neighbor coordination can be treated in an average way. Although our calculation is intended for amorphous alloys (no long-range periodicity is assumed), the results are also valid for crystalline alloys. This

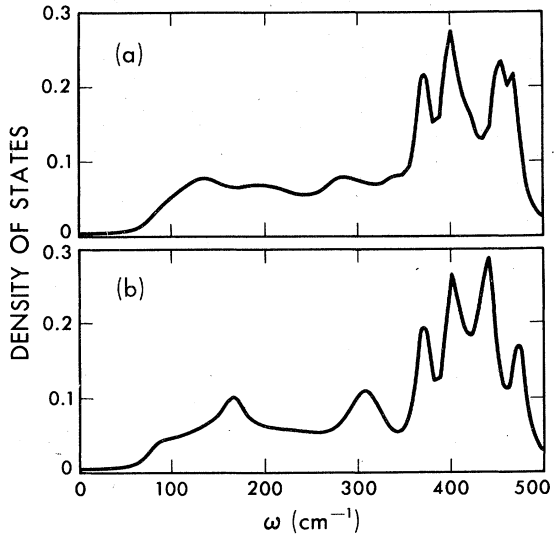

FIG. 9. Local density of states vs frequency associated with a Si atom for two different 17-atom clusters (see text). (a) The first-nearest-neighbors shell has two Si and two Ge atoms, and the atom distribution in the second-nearest-neighbors shell is random. (b) All the atoms are surrounded by two of its own kind and two of the other kind. A small (8 cm^{-1}) imaginary contribution to the frequency has been added.

stresses again the importance of short-range order in these alloys.

(ii) Good agreement between theory and experiments indicates that the unknown matrix elements in Raman scattering do not introduce spurious structure in the density of states.

(iii) Distribution of Si and Ge atoms is essentially random. Study of possible deviation from the random distribution would require us to analyze larger clusters or else to go beyond the mean-field approximation in the boundary of small clusters. This possibility is currently being analyzed.

(iv) In spite of its simplicity, the Born model seems to be appropriate to study amorphous Si_xGe_{1-x} alloys given the experimental resolution.[6]

(v) The model we propose assumes perfect tetrahedral bonding and neglects effects due to the presence of closed rings of bonds. Effects of bond angle variations and topology should be investigated.

In conclusion, in spite of the simplicity of our model, all the features of the Raman spectra are reproduced in our calculation. We believe that the outstanding properties, i.e., short-range order and tetrahedral coordination, of Si_xGe_{1-x} alloys are properly incorporated in our model.

---

*Address for the 1976–77 academic year: Instituto de Física del Estado Sólido [CSIC (Consejo Superior de Investigaciones Cientificas) and UAM], Universidad Autônoma, Cantoblanco, Madrid 34, Spain.

†Work supported by the NSF through Grant No. DHP72-03106-A02.

[1]See, for instance, AIP Conf. Proc. (to be published).

[2]M. Gorman and S. A. Solin, Solid State Commun. 15, 761 (1974).

[3]G. Lukovsky, F. L. Galeener, R. C. Keezer, R. H. Geils, and H. A. Six, Phys. Rev. B 10, 5134 (1974).

[4]M. H. Brodsky, in *Light Scattering in Solids*, edited by M. Cardona (Springer, Berlin, 1975).

[5]J. S. Lannin, in *Amorphous and Liquid Semiconductors*, edited by J. Stuke and W. Breing (Taylor and Francis, London, 1974).

[6]J. S. Lannin, Solid State Commun. 19, 35 (1976).

[7]R. Alben, D. Weaire, J. E. Smith, and M. H. Brodsky, Phys. Rev. B 11, 2271 (1975).

[8]P. Dean, Rev. Mod. Phys. 44, 127 (1972); D. Beeman and R. Alben, AIP Conf. Proc. (to be published).

[9]R. J. Elliott, J. A. Krumhansl, and P. L. Leath, Rev. Mod. Phys. 46, 465 (1974).

[10]G. Lucovsky and R. M. Martin, J. Non-Cryst. Solids 8/10, 185 (1972).

[11]A. S. Barker, Jr., and A. J. Sievers, Rev. Mod. Phys. Suppl. 47, 2 (1975).

[12]F. Yndurain, Phys. Rev. Lett. 37, 1062 (1976).

[13]L. M. Falicov and F. Yndurain, Phys. Rev. B 12, 5664 (1975).

[14]J. D. Joannopoulos and F. Yndurain, Phys. Rev. B 10, 5164 (1974).

[15]J. D. Joannopoulos and M. L. Cohen, Solid State Phys. 31 (1976).

[16]N. J. Shevchik, J. S. Lannin, and J. Tejeda, Phys. Rev. B 7, 3987 (1973).

[17]M. Born and K. Huang, *Dynamical Theory of Crystal Lattices* (Oxford University, New York, 1954).

[18]F. Yndurain and P. N. Sen, Phys. Rev. B 14, 531 (1976).

[19]M. F. Thorpe, J. Phys. C 7, 4037 (1974).

[20]V. T. Rajan and F. Yndurain, Solid State Commun. 20, 309 (1976).

[21]D. W. Feldman, M. Ashkin, and J. H. Parker, Jr., Phys. Rev. Lett. 26, 642 (1971).

[22]J. E. Smith, Jr., M. H. Brodsky, B. L. Crowder, M. I. Nathan, and A. Pinczuk, Phys. Rev. Lett. 26, 642 (1971).

[23]R. A. Logan, J. M. Rowell, and F. A. Trumbore, Phys. Rev. 136, 1751 (1964).